Naval Research Laboratory

Stennis Space Center, MS 39529-5004

NRL/MR/7180--05-8872

Subcritical Acoustic Penetration into Sandy Sediments with Negligible Interface Roughness

ROGER W. MEREDITH
STEVE STANIC
EDGAR T. KENNEDY

Acoustic Simulation, Measurements, and Tactics Branch
Acoustics Division

BRIAN HOUSTON
HARRY SIMPSON

Physical Acoustics Branch
Acoustics Division

June 6, 2005

REPORT DOCUMENTATION PAGE

Form Approved
OMB No. 0704-0188

1. REPORT DATE *(DD-MM-YYYY)*	2. REPORT TYPE	3. DATES COVERED *(From - To)*
06-06-2005	Memorandum Report	

4. TITLE AND SUBTITLE

Subcritical Acoustic Penetration into Sandy Sediments with Negligible Interface Roughness

5a. CONTRACT NUMBER

5b. GRANT NUMBER

5c. PROGRAM ELEMENT NUMBER
62435N

6. AUTHOR(S)

Roger W. Meredith, Steve Stanic, Edgar T. Kennedy, Brian Houston,* and Harry Simpson*

5d. PROJECT NUMBER

5e. TASK NUMBER

5f. WORK UNIT NUMBER

7. PERFORMING ORGANIZATION NAME(S) AND ADDRESS(ES)

Naval Research Laboratory
Acoustics Division
Stennis Space Center, MS 39529-5004

Naval Research Laboratory
Acoustics Division
Washington, DC 20375-5350

8. PERFORMING ORGANIZATION REPORT NUMBER

NRL/MR/7180--05-8872

9. SPONSORING / MONITORING AGENCY NAME(S) AND ADDRESS(ES)

Office of Naval Research
800 North Quincy Street
Arlington, VA 22217-5660

10. SPONSOR / MONITOR'S ACRONYM(S)

11. SPONSOR / MONITOR'S REPORT NUMBER(S)

12. DISTRIBUTION / AVAILABILITY STATEMENT

Approved for public release; distribution is unlimited.

13. SUPPLEMENTARY NOTES

*Physical Acoustics Branch, Acoustics Division, Naval Research Laboratory, Washington, DC 20375-5350

14. ABSTRACT

Recent observations of anomalous subcritical penetration in sandy sediments has renewed interest in the physics of acoustic sediment interaction. This paper presents measurements conducted at subcritical grazing angles over the frequency range of 1-12 kHz and examines the effects of multipath arrivals on the bottom penetration. Broadband signals, over a frequency range of 500 Hz to 12 kHz, were transmitted from a fixed source tower into the sediment and were received on a buried hydrophone array. The array was repositioned sequentially in range to acquire signals with grazing angles of 28, 15, 8, 5, 4, 3, and 2 degrees. The direct-path penetration ratios measured here compared favorably with previous studies. For multipath propagation, it is shown that additional arrivals create significant variability in penetration ratio. The frequency regime associated with the evanescent wave was well defined at even the lowest grazing angles. Seismo-acoustic modeling using OASES 2.2 showed reasonable agreement out to about 7000 Hz for grazing angles of 28, 15, and 8 degrees. The penetration ratio using a second (buried) reference hydrophone yielded much improved model-data comparisons.

15. SUBJECT TERMS

Sediment penetration; Acoustics; Bottom scattering

16. SECURITY CLASSIFICATION OF:			17. LIMITATION OF ABSTRACT	18. NUMBER OF PAGES	19a. NAME OF RESPONSIBLE PERSON
a. REPORT	b. ABSTRACT	c. THIS PAGE			Roger W. Meredith
Unclassified	Unclassified	Unclassified	UL	32	19b. TELEPHONE NUMBER *(include area code)* (228) 688-5231

Standard Form 298 (Rev. 8-98)
Prescribed by ANSI Std. Z39.18

CONTENTS

SUBCRITICAL ACOUSTIC PENETRATION INTO SANDY SEDIMENTS WITH NEGLIGIBLE INTERFACE ROUGHNESS

I. Introduction

Observations of anomalous subcritical penetration in sandy sediments [1] has renewed interest in the physics of acoustic sediment interaction. Recent investigations into the role of surface roughness plays in scattering acoustic energy into the ocean sediment at grazing angles below critical have included simulation and modeling [2] and at sea measurements [3-6]. These results have quantified the inadequacy of the flat-interface model and identified interface roughness scattering as an important mechanism for acoustic penetration into the sediment at subcritical angles. Maguer et al.'s [7, 8] measurements and modeling show two distinct frequency regimes with 5-7 kHz as a transition band. At frequencies below 5-7 kHz, the evanescent wave dominates acoustic penetration in the first 0.5 m of depth. The evanescent wavenumbers penetrate only a few wavelengths into the sandy sediment and decay exponentially with depth. They are associated with wavefront curvature. [9]. Sediment-interface and sediment-volume scattering dominated the penetration ratio at frequencies above 5–7 kHz. Laboratory measurements have also been conducted. Lim et al. [10] placed polystyrene beads at the interface between two-fluids of different density and measured the acoustic transmission as a function of bead size over grazing angles of 14 to 37°. Their work clearly demonstrates that Bragg-consistent interface scattering produces energy transfer in the far field. Near the interface, Bragg-scattering components were difficult to assess because of near field effects at the scattering interface, multiple scattering.

This paper presents results of a series of acoustic ocean-sediment penetration measurements conducted at subcritical grazing angles over a relatively smooth interface in the frequency range of 1-12 kHz. It examines the effects of multipath arrivals (at different incidence

Manuscript approved July 30, 2004.

angles) on bottom penetration.

II. Acoustic Measurement System

This experiment was conducted by the Naval Research Laboratory, in July 2001, in St Andrews Bay, Panama City, FL. One objective of these experiment was to acquire sediment penetration measurements at subcritical grazing angles. Broadband signals were transmitted from a fixed location source into the sediment and were received on a buried hydrophone array. A G34 acoustic source was mounted 3.7 m above the seafloor and operated over a frequency range of 500 Hz to 12 kHz. A 4.5 second pulse was transmitted using a LFM with a low-frequency bandwidth of 500 - 5000 Hz and a high-frequency bandwidth of 5 -12 kHz. Corresponding beamwidths varied from omnidirectional at 1 kHz to approximately 35 deg at 10 kHz. The transmit pulse time series and spectra are shown in Figure 1 and a summary of important acoustic parameters appears in Table I.

The buried acoustic receiver was a 6-element, linearly-spaced hydrophone array with a 50 cm aperture. The array was buried vertically and repositioned sequentially in range to acquire signals with grazing angles of 28, 15, 8, 5, 4, 3, and 2 degrees. The signals from each hydrophone were cabled back to a moored ship, and a 12 ms time series was digitized at a sampling rate of 100 kHz and recorded. Sixty sequential pulses (at a 1 Hz repetition rate) were coherently averaged to remove any thermal microstructure effects.

III. Bottom Properties

Analysis of diver-collected cores taken along the axis from the acoustic source to the buried hydrophone array provided a measure of the physical properties of the sediment. Core

analysis was performed in 0.5 cm sections to a depth of 20 cm, and the results are given in Table II. Physical properties and sediment composition are irregular in both depth and range. Water content and porosity also vary with depth but are more uniform with range. The quantity of gravel is depth dependent, while sand and clay constituents are more persistent in both depth and range.

The compressional (phase) velocities of the core samples ranged from 1709 to 1749 m/sec (measured at 400 kHz). The grain size distribution spans 1.7–1.9 phi, the porosity varies from 42–50 %, and the sand composition ranges from 89–97 %. In-situ estimates of sediment phase velocity were made utilizing head wave propagation at 20 kHz over a 20 m range and produced a phase velocity of 1644 ± 40 m/s. The seismo-acoustic inversion technique, SAGA, [11] gave an estimate of 1720 m/s. The time delay with depth, of the phase of the received signals (for all available grazing angles), can be used to obtain an estimate of the critical angle if the buried hydrophone array tilt is known [7, 8]. For this data, assuming less than 10° tilt, the critical angle was estimated to be 27°, yielding a sediment speed of 1727 m/s. The sound speed in water, averaged from multiple CTD casts was 1538 ±1 m/s. Although no high-resolution measurements were made, the sediment interface was relatively smooth, having less than 1 cm roughness.

IV. Bottom Penetration Ratio Measurement Results

The penetration ratio is used as a means of quantifying sediment penetration and to facilitate comparisons of model results with experimental data. The penetration ratio is defined as the ratio of the pressure spectral density from a hydrophone buried in the sediment to a reference spectral density [7, 8]. The penetration ratio represents the pressure produced by unit amplitude

of the incident wave and is given by:

$$P_r(f)_{d,\alpha} \equiv \left| \frac{P_{sed}(f)_{d,\alpha}}{P_{ref}(f)_{\alpha}} \right|^2, \begin{cases} \text{f = frequency} \\ \text{d = sediment depth,} \\ \alpha = \text{grazing angle} \end{cases} \quad (1)$$

A negative dB value of penetration ratio indicates an attenuation of energy (absorption and scattering) relative to the reference phone. Scattering and reflections may give rise to positive dB values of the penetration ratio [7, 8]. For this work, the reference hydrophone is located at the water-sediment interface rather than 1 m above the interface.

IV.A. Direct Path Penetration Paths

This first section shows the results for three grazing angles, 28°, 15°, and 8° for which the direct path arrival has been time-gated out of the received signal. Figure 2 shows the individual time series for each buried phone at a 28° grazing angle. Although not shown, the matched filter output for each hydrophone (at both the 28° and 15° grazing angles) reveals that the peak intensity is displaced in sample lag with depth. The average moveout is approximately 10 milliseconds over the span of the buried array (0.5 m). This is larger than would be expected due to the vertical tilt of the array. For example, a ten degree tilt (away from vertical) in the buried array would generate a moveout on the order of 50 milliseconds. The acoustic travel time between array elements is masked by the array tilt, and therefore, only magnitudes are considered in this paper. The average attenuation, in dB/m, computed from the matched filter peak at each depth is given in Table III for each grazing angle along with the average penetration ratio magnitude computed from Eq. 1.

Figure 3 shows the magnitudes of the penetration ratio at grazing angles of 28°, 15°, and 8°. (The reference phone was positioned on top of the sediment interface.) At the shallower burial depths , for 28°, the penetration ratio value at lower frequencies is relatively constant. Above 7 kHz, the penetration ratio value decays slightly with frequency. Overall, the magnitude of the penetration ratio at 28° is a few dB lower than that of Maguer et al. [7, 8]. Overall, their data show two features, a linear falloff with frequency from 2 – 7 kHz followed by scalloping from 7-12 kHz. They showed that the linear falloff was associated with the evanescent wave, and the scalloping was associated with interface-roughness and sediment-volume scattering. For rough surfaces, the transmitted field is often modeled as the sum of a coherent portion and an incoherent portion [12, 13, 2]. For long acoustic wavelengths relative to the roughness scale, the incoherent term is negligible, for shorter wavelengths, the incoherent term plays a more substantial role. For the data presented here, the overall roughness scale that is lower than was the case in the earlier studies [7, 8]. Also, since large scalloping at the higher frequencies were not observed, the incoherent scattering component is small. At deeper burial depths (0.3, 0.4, 0.5 m), the scalloping or undulations associated with scattering begin at 1 kHz, and thus there is no detection of the evanescent wave. There are peaks in the penetration ratio near 3 and 6 kHz that are consistent at all depths that imply unusually high penetration (less loss). The depth consistency eliminates Bragg scattering from the interface as cause of the increased penetration and the incoherent scattering component is small .

Overall for the 15° data, the magnitude of the penetration ratio is, on average, the same as the 28° data or slightly higher. A linear falloff with frequency occurs only for the uppermost

phones and only out to about 3 kHz. Also, there is no scalloping at higher frequencies, just small undulations. The 15° data is significantly different due to two strong peaks (at different frequencies from the 28 ° data). One peak is near 4 kHz and one is near 10 kHz. These are the highest penetration ratio values (least loss) in the time-gated direct path data. The individual peak shapes and widths are suggestive of resonance, but the multiple number of peaks may be more indicative of scattering over a large range of ka values [12].

The magnitude of the penetration ratio for the 8° grazing angle is about 10 dB lower than for 28° and 15° as would be expected by the smaller grazing angle. The 8° data show a linear falloff with frequency that is characteristic of the evanescent wave [7, 8]. The shallower depths show the decay out to only 3 kHz, but for the deeper phones the decay is linear out to nearly 10 kHz before undulations due to scattering become significant. The signal-to-background level of the penetration ratio was examined using small segments of the received signals just prior to the first arrival and are consistent with the inverse of the source spectrum. Below 1000 Hz, the average signal-to-background level is typically 10 dB. From 1000 - 8000 Hz the the average signal-to-background level increases linearly with a slope of 20 dB per octave and from 8000-12000 Hz the the average background level is relatively constant hovering around 50 dB. Overall, the time-gated direct-path results for these grazing angles compares favorably with the benchmark study [7,8] except for the occurrence of the peaks in the 28° and the 15° data.

IV.B. Direct Path and Multipath Comparison

Figure 4 compares the time-gated direct-path penetration ratios of Fig. 3 with the received signals containing two additional arrivals (surface bounce and bottom-surface bounce) for grazing angles of 28°, 15°, and 8°. The corresponding surface reflected grazing angles (75°, 61°, and 42°)

are all greater than the critical angle. For 28°, the multipath effect on overall penetration ratio magnitude is relatively small (Fig. 4a). However, the variability of the penetration ratio magnitude as a function of frequency is noticeably less at all depths with the addition of multipaths. Changes in the penetration ratio as a function of hydrophone depth are noticeably less for the multipath case than for the time-gated direct-path case. The 3 kHz peak observed in the direct path data, is shifted lower in frequency to ~2.6 kHz for all depths and the peak near 5.8 kHz, is mostly obscured in the multipath data.

The 15° comparison of penetration ratio is the strongest indicator of anomalous subbottom penetration. The difference in penetration ratio with and without multipaths (ensemble averaged over all depths), is less than 0.5 dB and it is less than 0.3 dB if the 0.2 m depth data is ignored. The two strong peaks in the multipath penetration ratio almost perfectly align in both magnitude and frequency with the direct path penetration ratio. The peaks may be consistent with Bragg scattering since they do change in frequency with changing grazing angle [8, 10]. However, the different incident grazing angles due to the addition of multipaths should show a shift or in frequency or at least a peak broadening (relative to the direct-path only) which are not observed. The high peak magnitude suggests a reflection. Another possibility for this anomaly exists in the sediment core data. Since both water content and composition of gravel vary with depth, perhaps an undetected gas or gravel pocket may be present. The biggest differences in penetration ratio for this grazing angle occur in the upper two hydrophones and in the evanescent wave portion of the frequency spectrum from 1-5 kHz [7, 8]. Here, the inclusion of the multipaths yields significantly less attenuation (higher penetration ratio magnitudes) than for the direct path only.

The 8° grazing angle penetration ratio comparison with and without multipaths shows the expected result. Multipaths fill in deep nulls, smooth the peaks, and reduce variability with frequency in the penetration ratio. With multipath returns included, the penetration ratio magnitude was higher and the difference (relative to the direct path penetration ratio) increased as depth increased (3 dB at 0.2 m depth and 10 dB at 0.5 m). The multipath penetration ratio shows a small peak near 2.4 kHz, that was not observed in the direct path data. This peak is also constant in depth and corresponds with the peak in the penetration ratios for 28° but not for 15°. The 2-4 kHz band corresponds a scattering radius on the order of 10-20 cm, orders of magnitude larger than grain size but appropriate for an ensemble of sand dollar debris, which are known to exist in the area [3].

IV.C. Very Low Grazing Angle Multipath Penetration Ratios

This section compares the multipath penetration ratio for very low grazing angles of 5°, 4°, 3°, and 2° for which the direct-path cannot be time-gated. Results of penetration ratio versus depth and grazing angle are shown in Figure 5. Each penetration ratio includes the number of multipaths given in Table III. It should be noted that for these very small grazing angles, sound speed profile fluctuations, especially near the bottom, can alter the ray path yielding different grazing angles than expected by 1-2 ° [14]. One noticeable feature in these plots, but especially at the two deeper depths, is the pair of narrowband peaks at 730 and 1200 Hz that correspond to sharp nulls in the transmit waveforms and are essentially ratios of hydrophone noise.

The 5° results show the same constant peak at 4 kHz that was associated with anomalous penetration in the 15° grazing angle analysis. This peak is not discernible at 4°, 3°, and 2° grazing

angles and the anomalous penetration ratio peak at 10 kHz (for the 15° grazing angle) is not observed. For 5°, the first surface-reflected path grazing angle is 31°, still above the critical angle while for the surface-reflected path for the 4°, 3°, and 2° the grazing angles are below critical (24, 19, and 17° respectively). When the surface-reflected path grazing angle drops below the critical angle, there is a corresponding drop in penetration ratio magnitude. Generally, the penetration ratio decreases with decreasing grazing angle and more so for the deeper hydrophones. Overall, the modeled results have much less variability in the penetration ratio magnitude (~2-4 dB) than does the data (~ 8 dB). It is not until the deepest depth, 0.5 m, that the penetration ratio magnitude separates out in grazing angle as would be expected from direct path results and the higher grazing angle multipath results. This indicates that energy at all frequencies for the low grazing angles is possibly being entrained or trapped in the upper 10-30 cm of sediment.

Overall, for grazing angles of 2°, 3°, and 4°, the penetration ratio magnitudes decrease with frequency from 1 kHz to about 6-8 kHz, although the slope, with multipath arrivals included, is not as steep as the direct path slope. For each grazing angle there are strong similarities in the frequency structure that are independent of depth. From 8-12 kHz, the penetration ratio magnitude is relatively flat with multiple undulations less than 5 dB, which are comparable to Maguer, et al., [7, 8] and also to the direct path data shown in Figure 3. These undulations are again identified with interface scattering since peak locations shift with grazing angle [3, 10].

V. Penetration Ratio Modeling Results

This section compares seismo-acoustic modeling results from OASES 2.2 [15] with the

experimental results for the very low grazing angle data. OASES is a horizontally-layered sesmio-acoustic propagation model employing wave number integration to compute the complex acoustics field over a rectangular grid in range and depth. The acoustic field is modeled as a superposition of two fields, one produced by sources in an environment with no boundaries and the other is an unknown field, determined by boundary conditions that satisfy the homogenous wave equation. OASES computes the depth-dependent Green's function for a selected band of frequencies and integrates to obtain the acoustic field [15, 16]. The model was configured to match the basic experimental geometry, environment, and source pulse characteristics. The data-model comparisons include both a fluid half-space (c = 1710 m/s), and a poro-elastic (Biot) half-space. The Biot parameters were determined in part from sediment cores and in part from inversion methods [17], A third model used in the data comparison is with a composite of the first two consisting of a thin 0.05 m fluid layer (c = 1710 m/s), over top the Biot half-space. At very low grazing angles, this sediment model yields a better comparison with the frequency structure of the measured penetration ratios. The penetration ratio as a function of frequency was computed for each depth and for each grazing angle. In order to simplify and summarize the comparisons for each grazing angle, an ensemble dB average was then computed over all depths for both measurement and model values.

V.A. Penetration Ratio

Figure 6 shows the depth-averaged penetration ratio as a function of frequency for the source-to-receiver ranges that correspond to the direct-path grazing angles of 5°, 4°, 3°, and 2° and include the multipaths given in Table III. The 5° degree data show general agreement with model predictions, but the structure of the measured penetration ratio tends to be more complex than the modeled penetration ratio over all frequencies. Even so, the measured multipath

penetration ratio shows consistent peaks at 4 an 6 kHz that are not indicated by modeling the sediment as half-spaces. These peaks, seen previously in Figures 3-6, are now attributed to variability in the sediment with depth. Except for some differences in level and frequency, the 5° layered sediment model and measurements show reasonable agreement.

Overall, the low grazing angle multipath measurements reported here separate into two groups based on the grazing angle of the second arrival. When above critical, the multipath data are similar to that shown for the 5° case and compare favorably to evanescent wave model predictions out to about 7-8 kHz [7, 8] using a layered sediment. The frequency slope of the measured and modeled penetration ratio are similar. When the surface-reflected arrival grazing angle decreases below critical, the measurements show significantly less agreement with modeling. The difference magnitude between the measured and modeled penetration ratio is likely related to scattering losses in the measurements not accounted for accurately in the modeling.

The 4 °, 3 °, and 2 ° penetration ratio measurements have order 10 dB greater penetration loss than the higher grazing angle measurements. These penetration ratios also show poor agreement with model results over the entire frequency band. Overall, the measurements show 10-15 dB greater loss than predicted by the various sediment models. Although the penetration ratio values do not match, the combination sediment model (a thin fluid layer overlaying a Biot layer) better matches the overall frequency structure of the penetration ratio. For the 3° grazing angle a peak in the penetration ratio occurs near 8 kHz in both the measurement and model. Two measurements were taken at a 2° grazing angle. The geometry was identical in both measurements which took place 24 hours apart, after a complete tidal cycle. The first measurement is shown in black squares, the second in grey. These two measurements show consistent results except near

7 kHz. This difference could be due to a small change in water depth from tide stage, or small temperature changes from solar heating .

V.B. Post Penetration Ratio

The depth-averaged measurement-modeling comparisons in Fig. 6 show no satisfactory agreement for these very low grazing angles. A second penetration ratio was computed using the shallowest buried phone (0.10 cm) as the reference. This ' buried' or post-penetration ratio represents the acoustic pressure produced by an incident acoustic wave originating inside the sediment, thus the first-order effects of the interface scattering are eliminated from the ratio since the interface lies above the new reference phone location. A comparison of the ratio definitions are shown in Fig. 7.

The post-penetration ratios (computed with the buried reference) are shown in Fig. 8, again using an ensemble dB average over depth to summarize the dependence on grazing angle and reduce the variability inherent in sediment properties and composition. For the 5° result, the overall penetration ratio magnitude is about 3-5 dB lower (more loss) than for the original penetration ratio (Fig. 6). This difference must be due to scattering near the sediment interface. For the 1 - 6 kHz band, associated with the evanescent wave, the slope of the two penetration ratios with frequency are nearly identical for all grazing angles. For 5° the peak locations are also nearly identical while for the lower grazing angles the peak locations are slightly shifted between the two penetration ratios. Above the 6 kHz band, associated with scattering, some peak locations are shifted and some are constant.

The model-data comparisons for the post-penetration ratio show much improved

agreement at these very low grazing angles In the 1-5 kHz region, the post-penetration ratio structure and magnitude shows improved agreement with the sediment models and the layered model provides the best overall agreement with the measurements. At higher frequencies, the post-penetration ratio measurements still show more loss than indicated by the sediment models but the variability in magnitude is in better agreement with the models. The conclusion is that scattering at the water-sediment interface and in the first 0.1 cm of the sediment is the primary cause of the mismatch in penetration ratio levels between the measurements and sediment models at very low grazing angles shown in Fig. 6, even for this relatively smooth interface.

VI. Summary and Conclusions

The penetration ratio is a valuable tool for sediment propagation analysis. The direct-path penetration ratios measured here compared favorably with previous studies, except for the anomalies that was especially obvious at the 15° grazing angle. The Bragg-scattering component of the transmitted acoustic field was difficult to assess in part because of the large insonified area and sediment variability in both depth and range. It was shown that the first few arrivals dominate the variability in penetration ratio. Only a couple of multipath returns are needed to fill in nulls and smooth the undulations in the penetration ratio (Fig. 4). The grazing angle of the second arrival played a dominant role in the penetration ratio level. When the grazing angle for the second arrival went below critical, a significant drop in penetration ratio was observed.

The portion of the spectrum associated with the evanescent wave was well defined at even the lowest grazing angles. Higher variability was observed at lower grazing angles. Although the role of sediment variability was not well quantified, it clearly played a role in the variability. Out-of plane scattering and multiple-scattering may be a cause of variability at the lowest grazing

angles.

Siesmo-acoustic modeling using OASES 2.2 showed showed reasonable agreement in the evanescent frequency regime out to about 7000 Hz for grazing angles of 28, 15, and 8° using both fluid and Biot bottom models. For the grazing angles with subcritical grazing angles for the second arrival (4, 3, 2°), the composite layer bottom model provided a better match to measurements. The post-penetration ratio using a buried reference hydrophone yielded much improved model-data comparisons and verified that interface and sediment scattering are the likely source of the data -model mismatch .

ACKNOWLEDGMENTS

The authors would like to thank Henrik Schmidt, (MIT) for his gracious support and help with the OASES modeling, and Nickolas Chotiros and Marcia Issacson (ARL/UT) for several helpful ideas and suggestions. This work was supported by ONR under PE 62435N.

References

[1] N.P. Chotitros, " Biot model of sound propagation in water-saturated sand," J. Acoust. Soc. AM., 97, (1) 199-214, March 1995.

[2] E. I. Thorsos, D.R. Jackson, K.L William, " Modeling of subcritical penetration into sediments due to interface roughness," J. Acoust. Soc. AM., 107 (1), 263-277, 2000.

[3] E. I. Thorsos, et al., "An Overview of SAX99: Acoustical Measurement", IEEE Journal of Oceanic Engineering, Vol. 26, No. 1, January 2001

[4] M. D. Richardson, et al., "An Overview of SAX99: Environmental Considerations", IEEE Journal of Oceanic Engineering, Vol. 26, No. 1, January 2001

[5] D.R. Jackson, et al., "High frequency subcritical acoustic penetration into a sandy sediment," IEEE Journal of Oceanic Engineering, Vol. 27, No. 3, 346- 361, July 2002

[6] H. J. Simpson and B. H. Houston, "Synthetic array measurements of acoustical waves propagation into a water-saturated sandy bottom for a smoothed and roughened interface," J. Acoust. Soc. AM., 107 (5), 2329-2337, May 2000

[7] Alain Maguer, Warren L.J. Fox, Henrick Schmidt, Eric Pouliquen, and Edward Bovio, "Mechanisms for subcritical penetration into a sandy bottom: Experimental and modeling results," J. Acoust. Soc. AM., 107 (3), 1215-1225, March 2000.

[8] Alain Maguer, Edward Bovio, Warren L.J. Fox, Henrick Schmidt, "In situ estimation of sediment sound speed and critical angle," J. Acoust. Soc. AM., 108 (3), Pt. 1., 987-996, Sept. 2000.

[9] F. B. Jensen, W. A. Kuperman, M. B. Porter, and H. Schmidt, Computational Ocean Acoustics, Springer-Verlag, New York, 2000.

[10] R. Lim, I.C. Paustian, and J. L. Lopes, "Acoustic transmission across a roughened fluid-fluid interface," J. Acoust. Soc. AM., 109 (4), 1367-1383, April 2001

[11] Peter Gerstoft, private communication using Seismo-Acoustic inversion using genetic algorithms (SAGA), April 2002.

[12] H. Medwin ad J. D. Hagy, Jr., " Helmholtz-Kirchhoff theory for sound transmission through a statistically rough lance interface between dissimilar fluids," J. Acoust. Soc. AM., 51 (3), Pt. 2., 1083-1090, 1972.

[13] V.I. Tatarskii and M. Charnotskii, " Universal behavior of scattering amplitudes, for scattering from a plane in an average rough surface for small grazing angles," Waves in Random Media, 8, 29-40, 1998.

[14] H. Boehme, N.P. Chotiros, et al., "Acoustic backscattering at low grazing angles from the ocean bottom. Part I. Bottom backscattering strength," J. Acoust. Soc. AM., 77 (3), Pt. 1., 962, March 1985.

[15] Henrik Schmidt, "OASES Version 2.2 User Guide and Reference Manual," Massachusetts Institute of Technology. Cambridge, MA 1999.

[16] Henrik Schmidt and Finn B. Jensen, "A full wave solution for propagation in multilayered viscoelastic media with application to Gaussian beam reflection at fluid-solid interfaces," J. Acoust. Soc. AM., 77 (3), Pt. 1., 813-824, March 1985.

[17] Marcia Issackson and Nick Chotiros, private communication, August 2001.

Table I. Summary of acoustic parameters.

Acoustic Parameters	
Pulse type	LFM
Signal frequency (kHz)	0.5-12
Pulse length (ms)	4.5
Signal-to-noise dB	>20
Grazing Angles (deg)	3 - 28
Beam pattern	broad cardiod
Source-receiver range (m)	5 - 60

Table II : Physical properties and composition from two sediment cores.

Physical Properties							
Depth Interval (cm)	Phase Velocity (m/s)	Water Content %	Porosity %	Avg.Grain Density (g/cc)	Wet bulk Density (g/cc)	Folk Value mean (phi)	Folk Value std.dev. (phi)
0-5	1733	37	50	2.7	1.9	1.9	0.6
5-10	1721	29	44	2.7	2.0	1.8	0.5
10-15	1743	29	43	2.6	1.9	1.8	0.5
15-17	1736	27	41	2.6	2.0	1.7	0.6
0-5	1721	31	45	2.6	1.9	1.8	1.0
5-10	1740	28	43	2.6	2.0	1.8	0.5
10-15	1749	34	47	2.6	1.9	1.8	0.6
15-20	1709	28	43	2.6	1.9	1.7	1.4

Physical Composition				
Depth Interval (cm)	GRAVEL (%)	SAND (%)	SILT (%)	CLAY (%)
0-5	0.3	95.7	0.8	3.2
5-10	0.6	96.9	0.3	2.2
10-15	0.2	96.9	0.6	2.3
15-17	0.8	96.1	0.7	2.4
0-5	0.8	93.4	1.9	3.8
5-10	0.4	96.6	0.6	2.4
10-15	0.8	95.1	0.8	3.2
15-20	4.2	89.5	2.1	4.3

Table III. Comparison of measured attenuation estimates.

Direct-path grazing angle degrees	Number of multipath arrivals	Matched Filter Peak Attenuation dB/m	Penetration Magnitude Average over depth and frequency dB/m
28	3	-10	-7
15	3	-2	-6
8	4	-7	-8
5	5	-5	-10
4	5	-14	-13
3	5	-33	-25
2	6	-27	-24
2	6	-24	-15

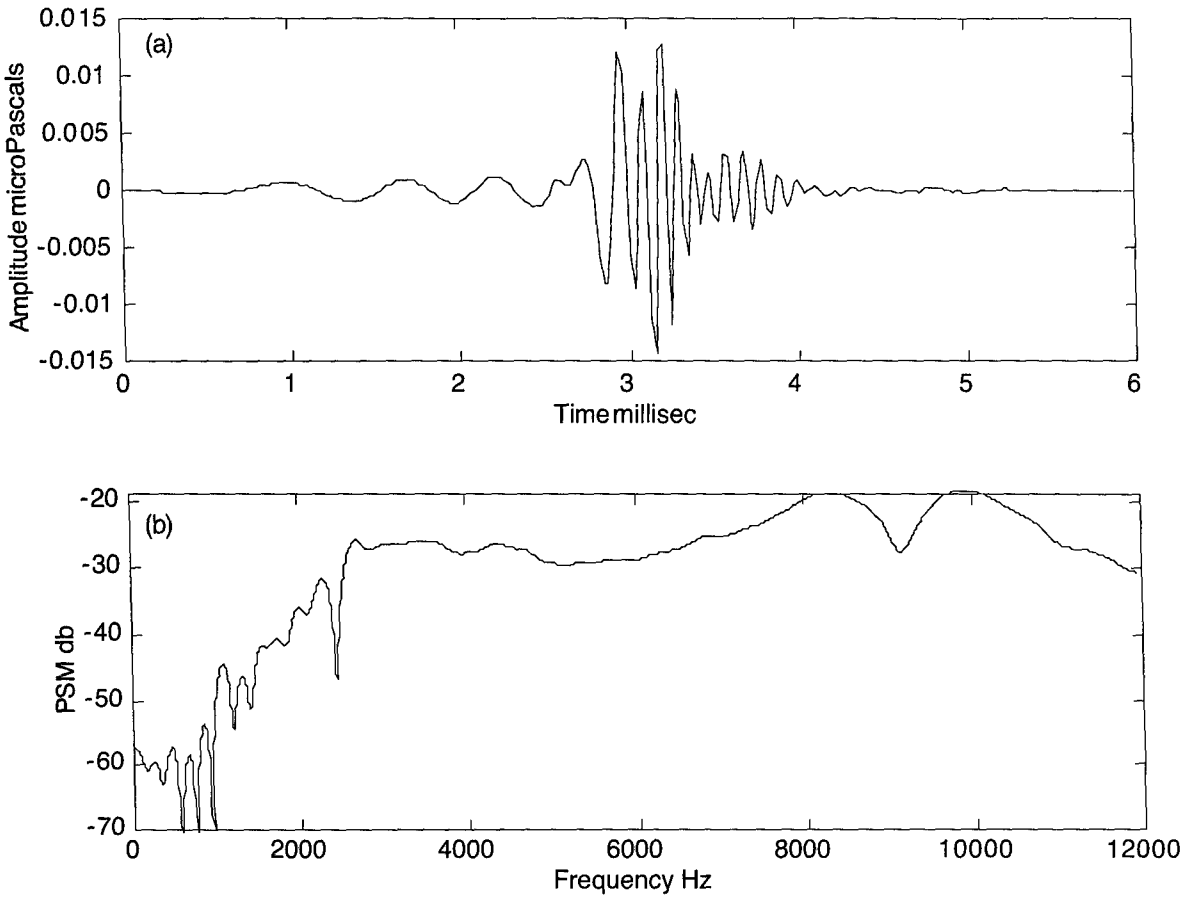

Figure 1. (a) Source pulse transmitted from the G34 and
(b) power spectral density magnitude.

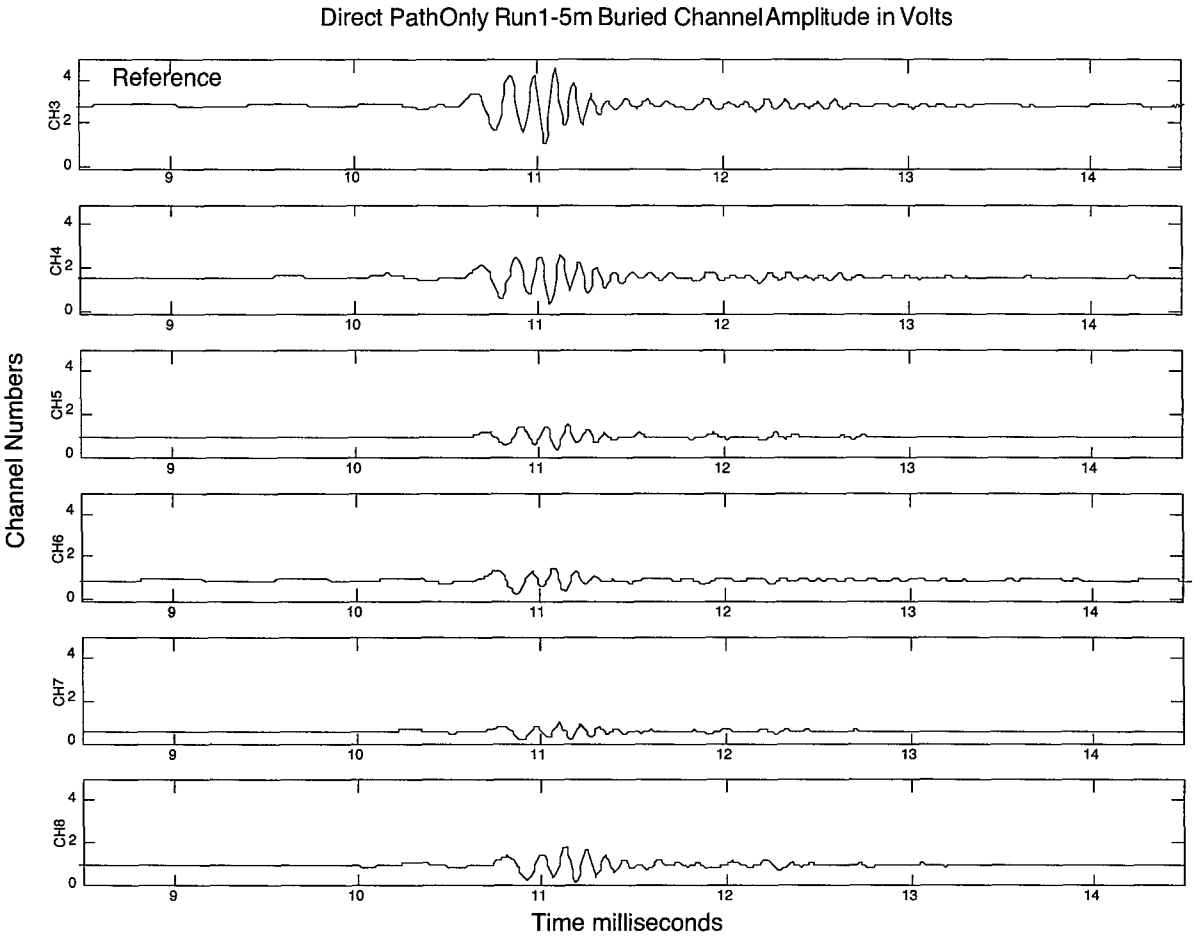

Figure 2. Direct Path (only) time series for individual buried phones and penetration ratios (magnitude) for a 28° grazing angle.

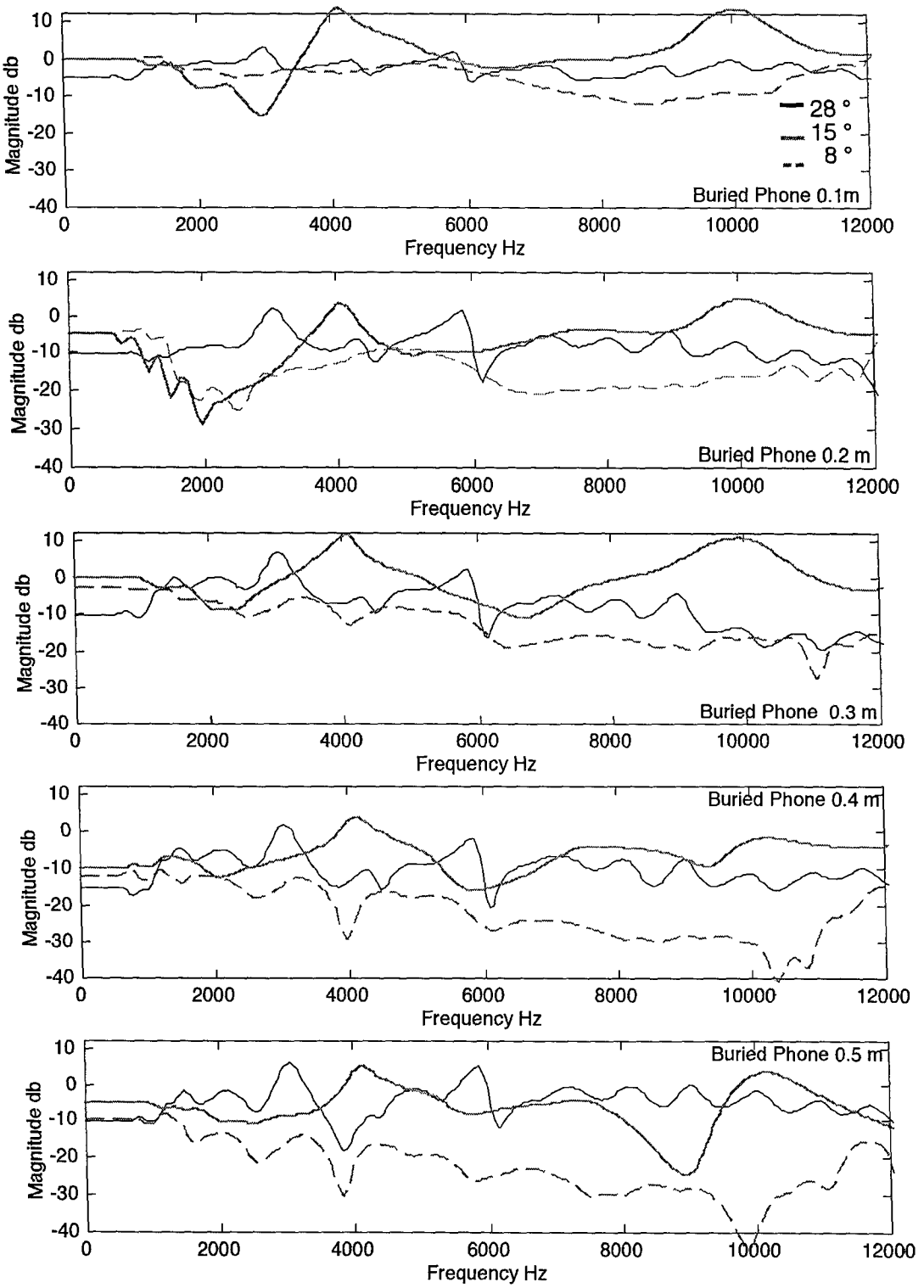

Figure 3. Penetration ratio in dB for the direct path signals at each of the buried phones for 28°, 15°, and 8° grazing angles.

(4a) 28 ° grazing angle

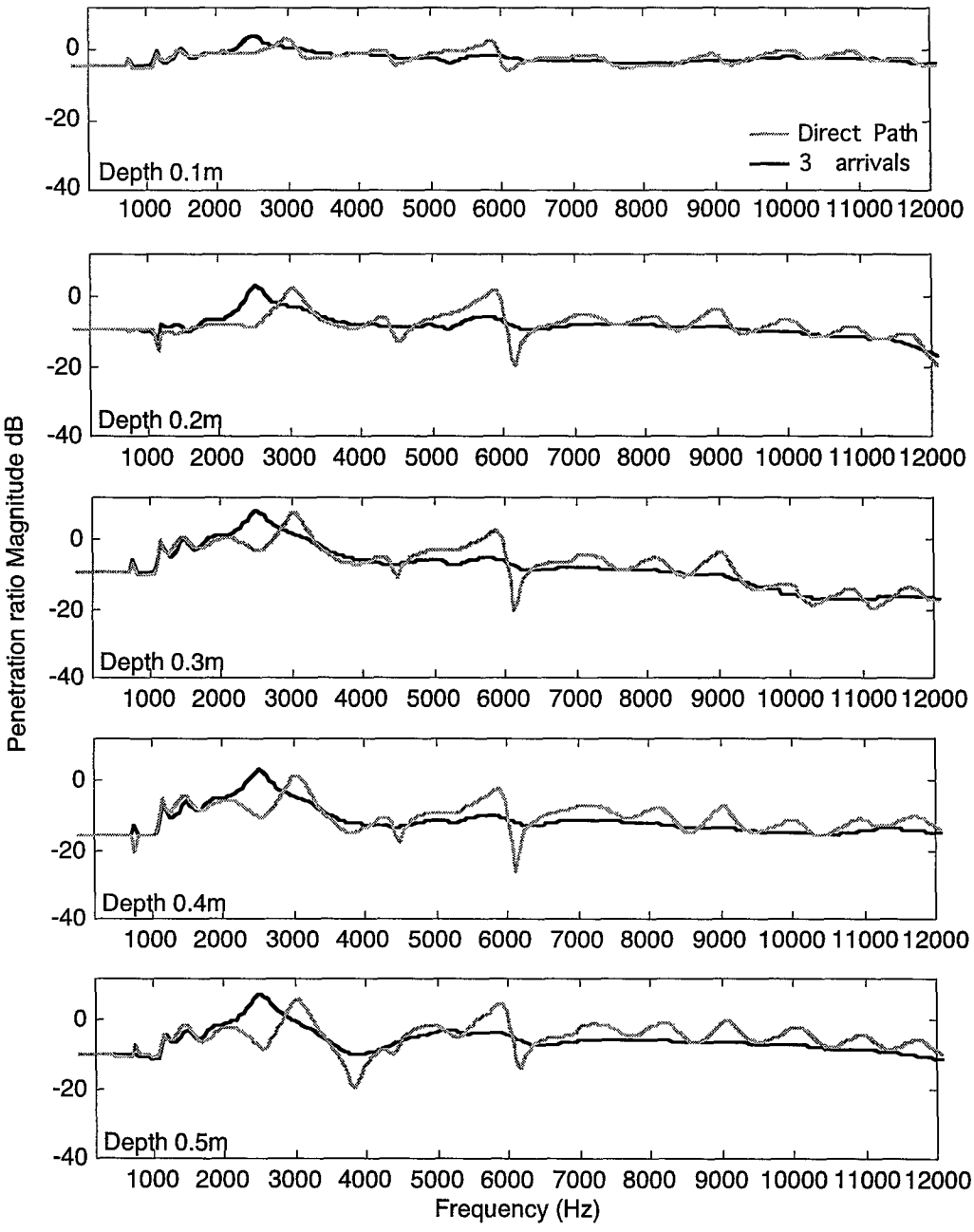

Figure 4. Comparison of penetration ratios of the direct path (only) and the direct path plus 2 or more multipaths. The direct path only penetration ratio is shown in grey.
(4a) 28°, (4b) 15°, and (4c) 8°.

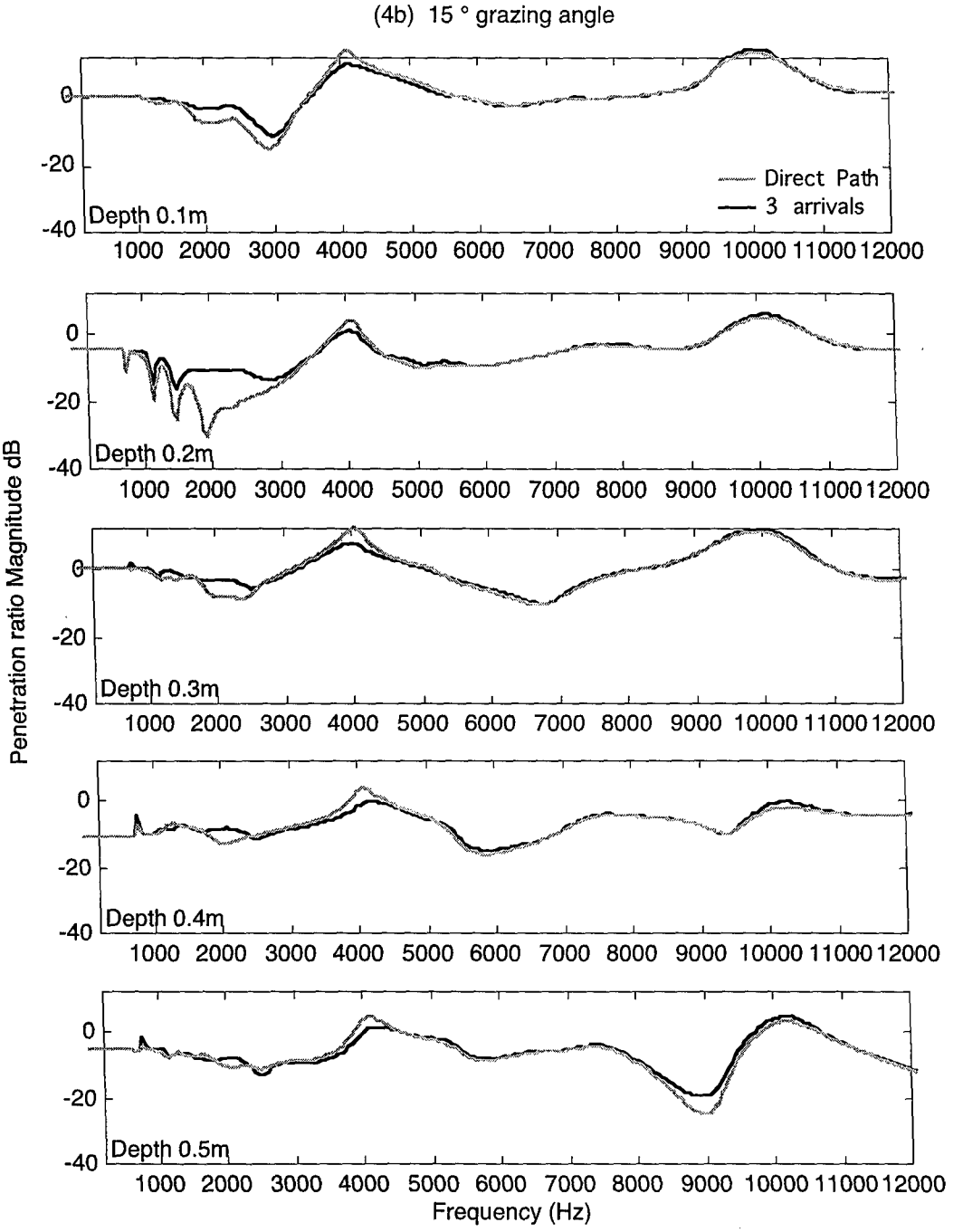
(4b) 15 ° grazing angle
Direct Path
3 arrivals
Depth 0.1m
Depth 0.2m
Depth 0.3m
Depth 0.4m
Depth 0.5m
Penetration ratio Magnitude dB
Frequency (Hz)
0
-20
-40
1000 2000 3000 4000 5000 6000 7000 8000 9000 10000 11000 12000

(4c) 8 ° grazing angle

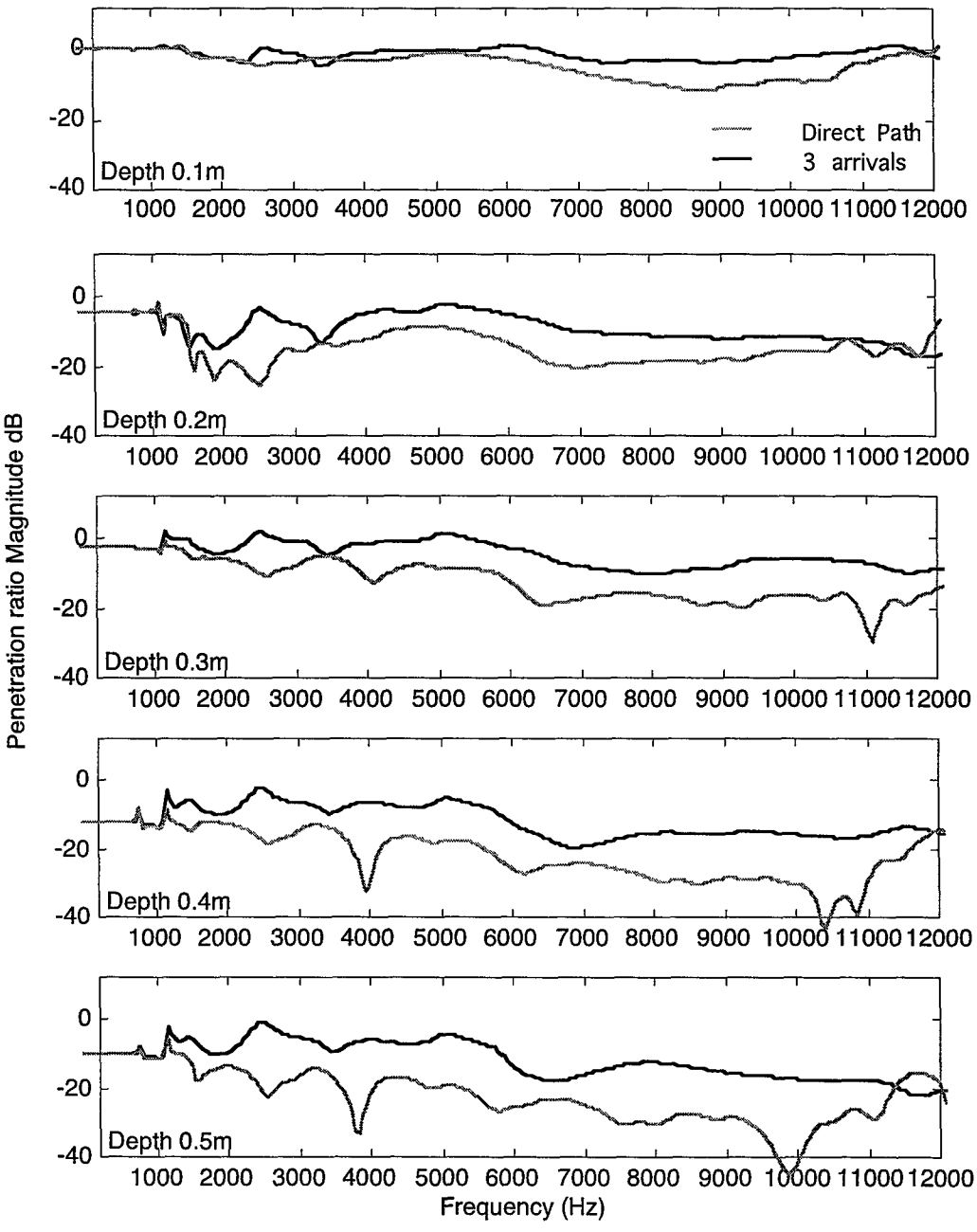

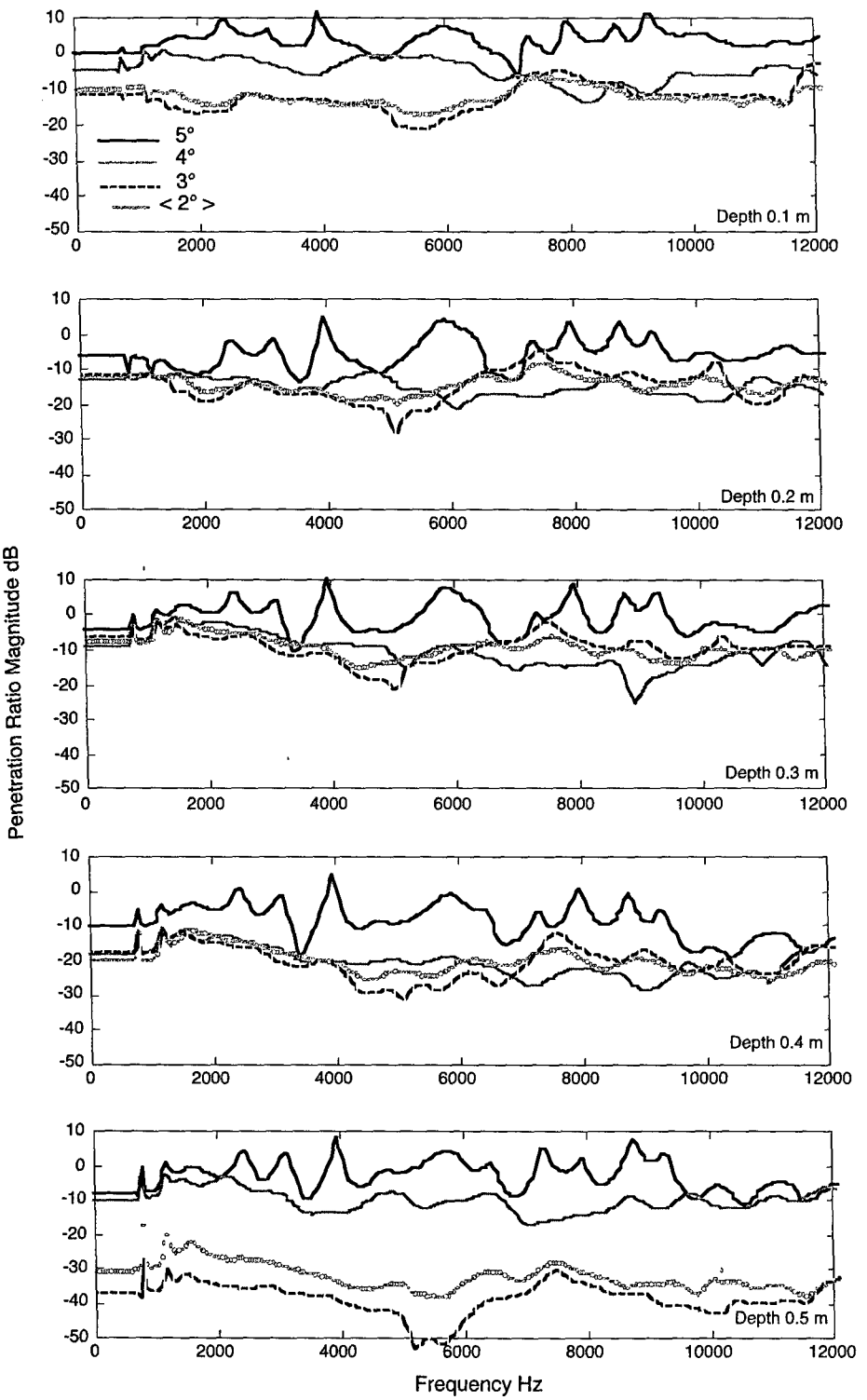

Figure 5. Penetration ratio in dB for the multipath arrivals at each of the buried phones for very low grazing angles.

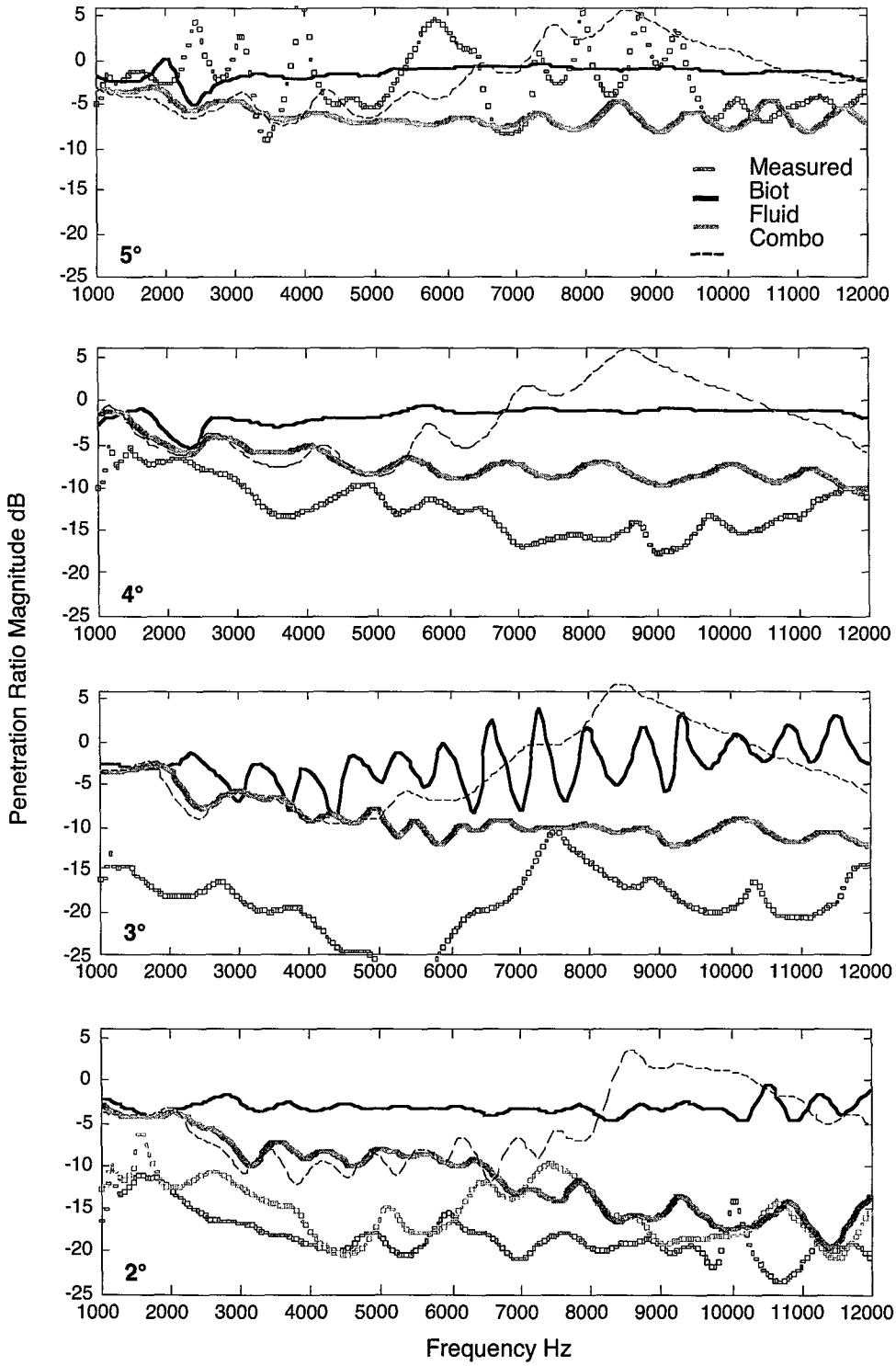

Figure 6. Penetration ratio (dB averaged over depths) for the multipath arrivals at each of the buried phones for very low grazing angles. The reference hydrophone is in the water column lying on top of the sediment. Two measurements were taken, 24 hours apart, corresponding to 2° grazing angle.

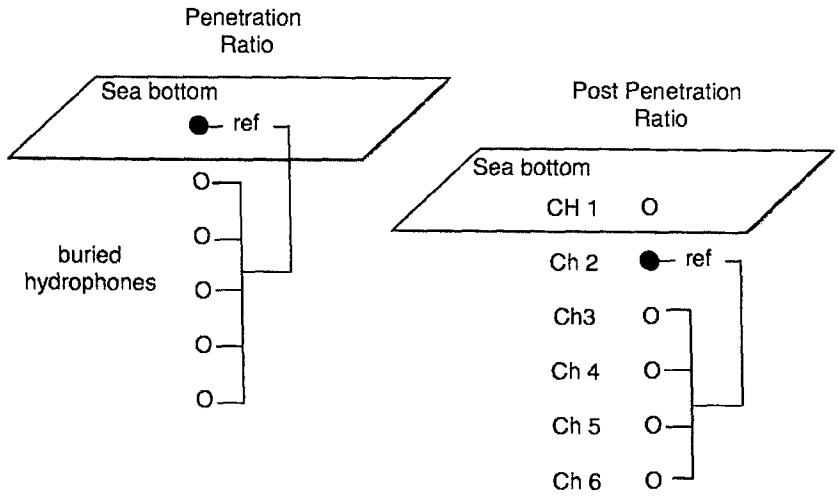

$$P_r(f) \equiv \left| \frac{P_i(f)}{P_{ref}(f)} \right|^2$$

Figure 7. Definition of penetration ratios.

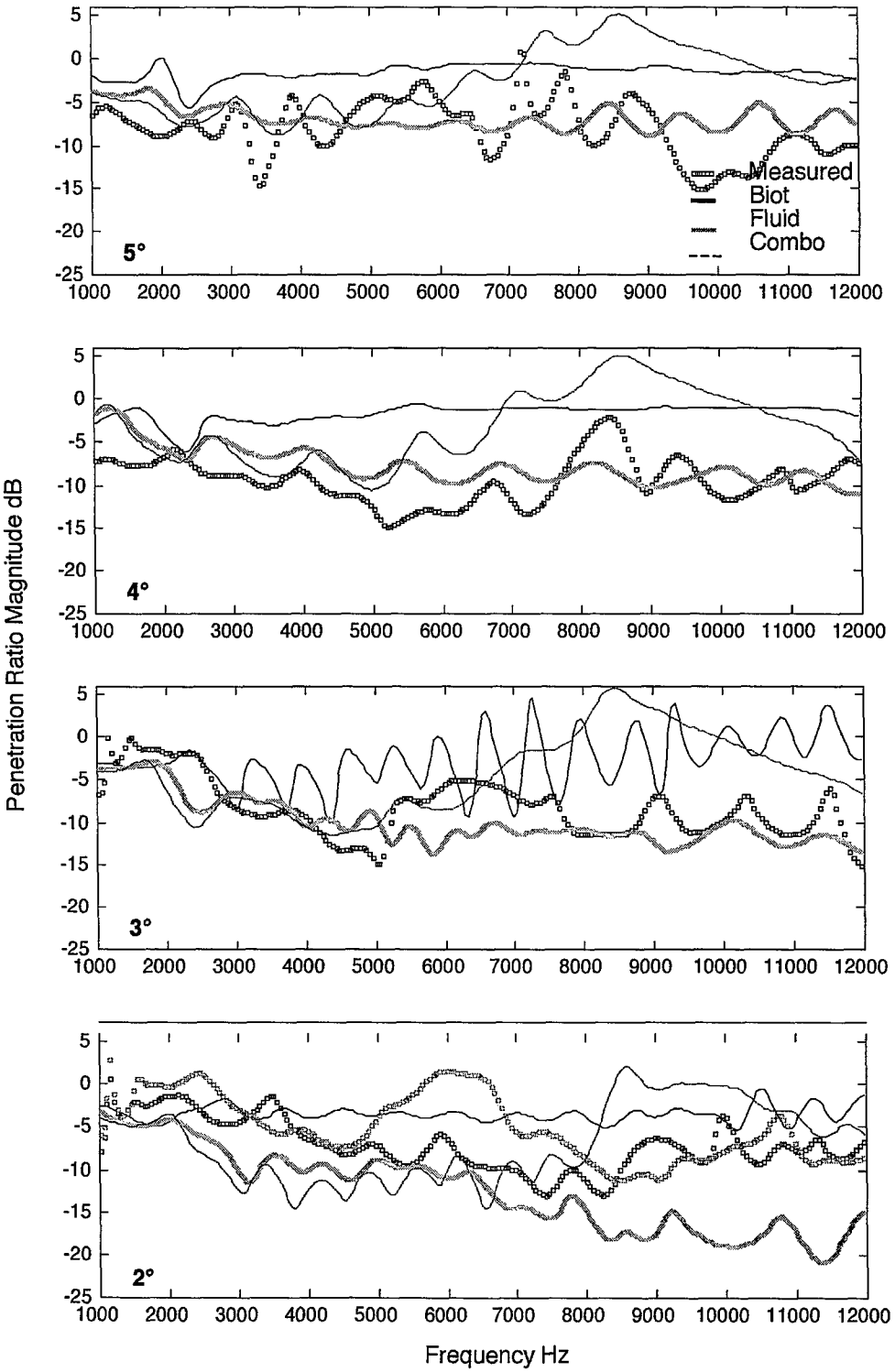

Figure 8. Penetration ratio (dB averaged over depth) for the multipath arrivals computed with buried hydrophone reference.